JOURNAL OF THEORETICAL AND APPLIED MECHANICS
63, 1, pp. 59-74, Warsaw 2025
https://doi.org/10.15632/jtam-pl/195695

LAYERED MECHANICS MODEL FOR SURFACE MOVEMENT AND DEFORMATION DUE TO CONFINED AQUIFER PUMPING

Liangliang Zhang

School of Civil Engineering and Architecture, Anhui University of Science and Technology, Huainan, 232001, PR China corresponding author e-mail: zllaust@163.com

Hua Cheng

School of Civil Engineering and Architecture, Anhui University of Science and Technology, Huainan, PR China and School of Resources and Environmental Engineering, Anhui University, Hefei, PR China

Surface movement and deformation caused by pumping from confined aquifers pose serious threats to safety and stability of surface buildings. A model for surface movement and deformation due to confined aquifer pumping is established based on the principle of coordinated strata deformation in which the effects of aquifer thickness, elastic modulus, pumping capacity, and overlying strata thickness are comprehensively considered. The model calculation results for surface subsidence caused by pumping from a confined aquifer in Dezhou City, Shandong Province, China, are compared with numerical simulation results to verify the accuracy and rationality of the model.

Keywords: confined aquifer; pumping well; layered mechanics; surface subsidence

1. Introduction

The long-term overexploitation of groundwater resources due to rapid urban development has resulted in decreasing groundwater levels and subsequent surface movement and deformation. This deformation seriously degrades the stability of the surface, which not only causes ground buildings to collapse and huge economic losses, but also serious damage to the natural environment and ecosystem (Loáiciga, 2013; Giang, 2022; Li *et al.*, 2021; Wang *et al.*, 2019). Surface subsidence was observed in Mexico City in 1891 (Ortega-Guerrero *et al.*, 1999). Overexploitation of groundwater in the Rafsanjan Plain in southeastern Iran has resulted in an annual subsidence rate of over 50 mm/year with local subsidence rates at some places exceeding 300 mm/year from 2006 to 2016. Since then, surface movement caused by groundwater pumping has been studied by researchers in the United States, Italy, Japan, and other countries (Abidin *et al.*, 2011; Holzer and Johnson, 1985). The identified land subsidence areas in China are mainly distributed in the Yangtze River Delta, North China Plain, and other regions, covering a total area exceeding 90000 km^2 (Cui and Tang, 2007).

Extensive in-depth research has been performed on ground subsidence caused by groundwater exploitation using two main types of methods (Xu *et al.*, 2015; Motagh *et al.*, 2017). In the first type, soil consolidation theory is used to calculate strata displacement and deformation caused by water loss in aquifers. Terzaghi proposed a well-known one-dimensional consolidation theory based on a series of assumptions and established the relationship between surface subsidence and time (Guido *et al.*, 2023). Giao (1997) proposed a subsidence calculation method based on one-dimensional consolidation theory combined with Green's theorem in which the dissipative pore water pressure is used as a variable. Peng *et al.* (2023) conducted

high-pressure long-term consolidation joint tests on the bottom aquifer of thick alluvial layers based on the ETAS test system, and studied the evolution law of the permeability coefficient.

The second type of methods for calculating surface movement and deformation during groundwater extraction is based on probability integration. Drawing on the theory developed for coal seam mining subsidence, the vertical compression of an aquifer caused by groundwater extraction is treated as a coal seam mining unit of varying thickness. The probability integration method is then used to calculate the surface subsidence based on random media theory (Malinowska *et al.*, 2020; Szojda and Kapusta, 2023). Tang and Bai (2011) analyzed the soil mechanics mechanism of water loss consolidation in saturated loess layers caused by mining and established a model for the additional surface subsidence deformation caused by water loss consolidation in the mining loess layers using random medium theory. Cheng *et al.* (2022) established a three-dimensional model for calculating surface movement and deformation under the combined action of a thick loose layer, thin-bedrock coal seam mining, and aquifer drainage using soil consolidation theory and random medium theory.

Although the two types of methods for calculating surface subsidence mentioned above have been widely applied in practical engineering, they still suffer from some shortcomings that need to be addressed. Consolidation theory models do not accurately reflect the surface subsidence changes in the entire aquifer water loss area while the probability integration methods do not account for the effects of physical and mechanical parameters and layered distribution characteristics of strata above an aquifer on surface movement and deformation. In this study, the influence of physical and mechanical parameters of each stratum is considered using layered mechanics to establish a model for surface movement and deformation caused by pumping in a confined aquifer. The influence of pumping capacity, aquifer thickness, aquifer elastic modulus, and overlying strata thickness on surface subsidence and horizontal movement are analyzed. This study provides a theoretical basis for safety assessment in surface buildings for groundwater extraction and environmental protection.

2. Surface movement and deformation model

Heavy industrial and residential water use has led to frequent overexploitation of confined aquifers in strata. Before water pumping, the overlying strata on a confined aquifer are jointly supported by pore water and the soil skeleton. The stress and deformation are in equilibrium. Pumping results in a gradual decrease of the pore water pressure. A portion of the soil pressure originally borne by pore water is transferred to the soil skeleton, resulting in an increase in the effective stress and consolidation deformation of the aquifer (Galloway and Burbey, 2011; Zhou *et al.*, 2010). The continuous development of this deformation upward causes surface movement and deformation. Although the original equilibrium state is broken by pumping, the collaborative soil deformation and stress redistribution in the formation cause the entire formation to eventually reach a new equilibrium state. The differences in permeability characteristics, physical and mechanical parameters, and thicknesses of the confined aquifer and overlying strata result in varying deformation transmission and development across different strata. Therefore, the strata can be regarded as a layered stratum for calculating surface movement deformation caused by pumping from a confined aquifer. In our model, the self-consolidation deformation caused by pumping from a confined aquifer is first calculated using layered mechanics. The deformation at the top of the aquifer is then used as a disturbance source at the bottom of the overlying strata to obtain the surface movement deformation caused by the deformation at the bottom of the overlying strata based on deformation coordination conditions at the soil interface.

In layered mechanics, the displacement and stress at any stratum depth can be represented by the surface displacement and stress (Bobileva, 2015)

$$\begin{Bmatrix} \overline{u}(\zeta,H) \\ \overline{w}(\zeta,H) \\ \dfrac{\overline{\sigma}(\zeta,H)}{E}H \\ \dfrac{\overline{\tau}(\zeta,H)}{E}H \end{Bmatrix} = \begin{bmatrix} A_{11} & A_{12} & A_{13} & A_{14} \\ A_{21} & A_{22} & A_{23} & A_{24} \\ A_{31} & A_{32} & A_{33} & A_{34} \\ A_{41} & A_{42} & A_{43} & A_{44} \end{bmatrix} \begin{Bmatrix} \overline{u}(\zeta,0) \\ \overline{w}(\zeta,0) \\ \dfrac{\overline{\sigma}_z(\zeta,0)}{E}H \\ \dfrac{\overline{\tau}_{zr}(\zeta,0)}{E}H \end{Bmatrix} \tag{2.1}$$

where $\overline{u}(\zeta,H)$, $\overline{w}(\zeta,H)$, $\overline{\sigma}(\zeta,H)$, and $\overline{\tau}(\zeta,H)$ are the Hankel integral transformation equations for the horizontal displacement, subsidence, normal stress, and shear stress of the strata at depth H, respectively; $\overline{u}(\zeta,0)$, $\overline{w}(\zeta,0)$, $\overline{\sigma}(\zeta,0)$, and $\overline{\tau}(\zeta,0)$ are the Hankel integral transformation equations for the horizontal displacement, subsidence, normal stress, and shear stress at the surface, respectively; ζ is the integral parameter variable; and E is the elastic modulus.

The matrix coefficients are given by

$$\begin{aligned}
&A_{11} = A_{44} = \cosh\eta + \frac{\eta\sinh\eta}{2(1-\mu)} \\
&A_{12} = -A_{34} = \frac{1}{2(1-\mu)}\left[(1-2\mu)\sinh\eta + \eta\cosh\eta\right] \\
&A_{13} = -A_{24} = \frac{1+\mu}{2(1-\mu)}\sinh\eta \qquad A_{14} = \frac{1+\mu}{2\eta(1-\mu)}\left[(3-4\mu)\sinh\eta + \eta\cosh\eta\right] \\
&A_{21} = -A_{43} = \frac{1}{2(1-\mu)}\left[(1-2\mu)\sinh\eta - \eta\cosh\eta\right] \\
&A_{22} = A_{33} = \cosh\eta - \frac{\eta\sinh\eta}{2(1-\mu)} \\
&A_{23} = \frac{1+\mu}{2\eta(1-\mu)}\left[(3-4\mu)\sinh\eta - \eta\cosh\eta\right] \\
&A_{31} = -A_{42} = -\frac{\eta^2}{2(1-\mu^2)}\sinh\eta \\
&A_{32} = \frac{\eta}{2(1-\mu^2)}(\sinh\eta - \eta\cosh\eta) \qquad A_{41} = \frac{\eta}{2(1-\mu^2)}(\sinh\eta + \eta\cosh\eta)
\end{aligned} \tag{2.2}$$

where $\eta = \zeta H$, μ is Poisson's ratio, and sinh and cosh are hyperbolic sine and cosine functions, respectively

$$\begin{aligned}
u(r,H) &= \int_0^\infty \overline{u}(\zeta,H)\zeta J_1(\zeta r)\,d\zeta \qquad & w(r,H) &= \int_0^\infty \overline{w}(\zeta,H)\zeta J_0(\zeta r)\,d\zeta \\
\sigma(r,H) &= \int_0^\infty \overline{\sigma}(\zeta,H)\zeta J_0(\zeta r)\,d\zeta \qquad & \tau(r,H) &= \int_0^\infty \overline{\tau}(\zeta,H)\zeta J_1(\zeta r)\,d\zeta
\end{aligned} \tag{2.3}$$

where J_0 and J_1 are the zeroth- and first-order Bessel functions, respectively; and $u(r,H)$, $w(r,H)$, $\sigma(r,H)$, and $\tau(r,H)$ are the horizontal displacement, subsidence, normal stress, and shear stress of the strata at a horizontal distance r and depth H.

The pumping process of a confined aquifer is shown in Fig. 1. The part above the aquifer are the overlying strata and that below the stable aquifuge layer. Pumping changes only the water level of the aquifer but does not affect the deformation of its lower strata. The deformation of the upper strata is only dependent on the elastic modulus, Poisson's ratio, and thickness. Let the thickness of the confined aquifer be H_0, the thickness of the overlying loose layer H_w, the radius of the pumping well r_0, the pumping influence radius R, and the pumping capacity Q. After the

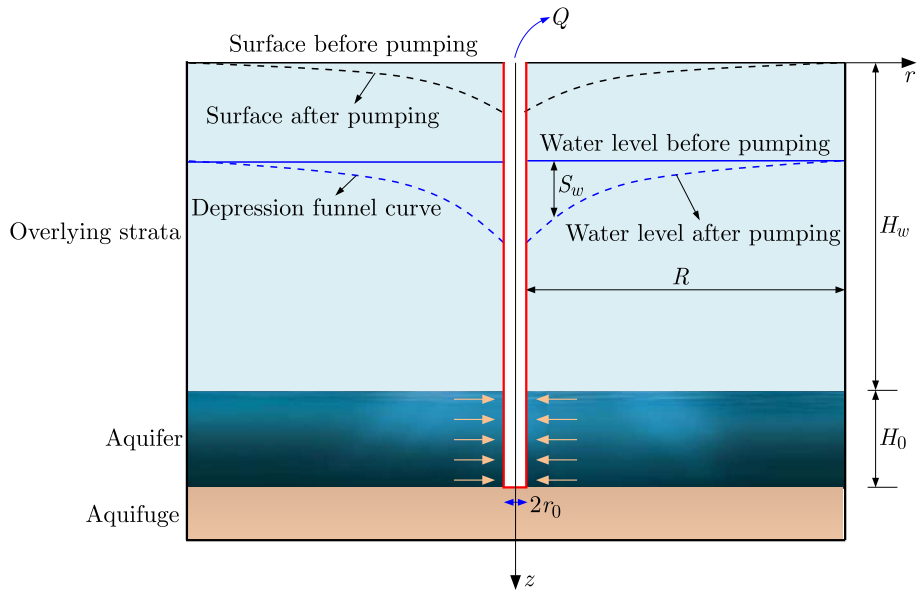

Fig. 1. Strata movement and deformation caused by pumping from a confined aquifer

pumping well has reached a stable state, the funnel curve of the confined water level drop can be expressed using the Dupuit formula (Bourel, 2024; Gamnitzer and Hofstetter, 2016)

$$s_w = \frac{Q}{2\pi k H_0} \ln \frac{R}{r} \tag{2.4}$$

where s_w is the depth of the water level drop and k is the permeability coefficient of the aquifer.

R is the pumping influence radius, which can be expressed using the Siechardt empirical formula (Jia *et al.*, 2016)

$$R = 10 s_w^{max} \sqrt{k} \tag{2.5}$$

where s_w^{max} is the maximum depth of the water level drop.

Focusing on the confined aquifer, the confined aquifer before pumping exerts a supporting force on the overlying strata with a magnitude directly proportional to the height of the confined water level. Pumping decreases the supporting force of the confined aquifer on the overlying strata and increases the effective stress of the soil (Liu *et al.*, 2023), which is directly proportional to the depth of the water level drop. This increase in the effective stress is equivalent to an additional load acting on the top of the aquifer with a funnel-shaped load distribution, which has the same funnel-shaped form as that of the aquifer level drop, as shown in Fig. 2.

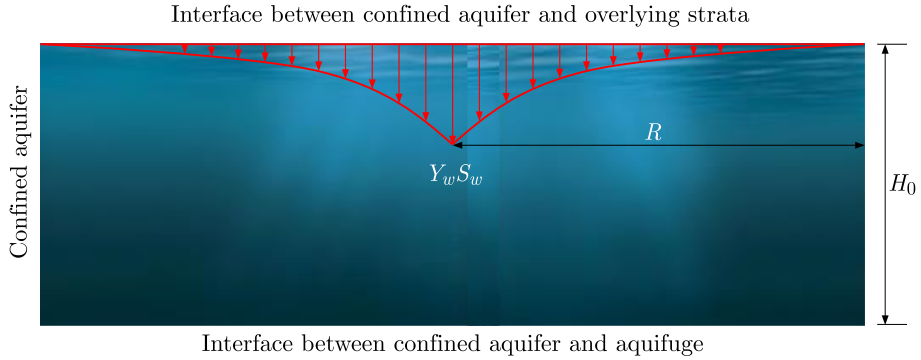

Fig. 2. Additional load acting on the top of the confined aquifer

The additional load at the top of the aquifer can be expressed as

$$\sigma_z(r, H_w) = \gamma_w s_w \qquad \tau_{zr}(r, H_w) = 0 \tag{2.6}$$

where γ_w is the weight of water and $\sigma_z(r, H_w)$ and $\tau_{zr}(r, H_w)$ are the normal and shear stresses acting on the top of the aquifer, respectively.

Substituting Eq. (2.6) into Eq. (2.3) yields

$$\overline{\sigma}_z(\zeta, H_w) = \int_0^R \gamma_w \left[\frac{Q}{2\pi k H_0} \ln \frac{R}{r}\right] r J_0(\zeta r)\, dr \tag{2.7}$$

where $\overline{\sigma}_z(\zeta, H_w)$ is the Hankel integral transformation of $\sigma_z(r, H_w)$.

It is generally believed that hydrophobic consolidation in an aquifer does not cause bottom deformation. The displacement at the aquifer bottom can therefore be assumed to be 0 (Jia *et al.*, 2016)

$$\overline{u}(\zeta, H_w + H_0) = 0 \qquad \overline{w}(\zeta, H_w + H_0) = 0 \tag{2.8}$$

where $\overline{u}(\zeta, H_w + H_0)$ and $\overline{w}(\zeta, H_w + H_0)$ are the Hankel integral transformation equations for the horizontal displacement and subsidence at the bottom of the confined aquifer, respectively.

By substituting Eqs. (2.7) and (2.8) into Eq. (2.1), the displacement and deformation at the top of the aquifer are obtained as follows

$$\begin{aligned} \overline{u}(\zeta, H_w) &= -\frac{A_{22}A_{13} - A_{12}A_{23}}{A_{11}A_{22} - A_{12}A_{21}} \times \frac{\overline{\sigma}_z(\zeta, H_w)}{E_2} H_0 \\ \overline{w}(\zeta, H_w) &= \frac{A_{21}A_{13} - A_{11}A_{23}}{A_{11}A_{22} - A_{12}A_{21}} \times \frac{\overline{\sigma}_z(\zeta, H_w)}{E_2} H_0 \end{aligned} \tag{2.9}$$

where E_2 is the elastic modulus of the confined aquifer and $\overline{u}(\zeta, H_w)$ and $\overline{w}(\zeta, H_w)$ are the Hankel integral transformation equations for the horizontal displacement and subsidence at the top of the confined aquifer, respectively.

Substituting Eq. (2.9) into Eq. (2.3) yields the horizontal displacement $u(r, H_w)$ and subsidence $w(r, H_w)$ at the top of the aquifer as follows

$$\begin{aligned} u(r, H_w) &= \int_0^\infty -\frac{A_{22}A_{13} - A_{12}A_{23}}{A_{11}A_{22} - A_{12}A_{21}} \times \frac{\overline{\sigma}_z(\zeta, H_w)}{E_2} H_0 \zeta J_1(\zeta r)\, d\zeta \\ w(r, H_w) &= \int_0^\infty \frac{A_{21}A_{13} - A_{11}A_{23}}{A_{11}A_{22} - A_{12}A_{21}} \times \frac{\overline{\sigma}_z(\zeta, H_w)}{E_2} H_0 \zeta J_0(\zeta r)\, d\zeta \end{aligned} \tag{2.10}$$

Equation (2.10) expresses the deformation at the top of the confined aquifer caused by pumping. According to the principle of deformation coordination, the displacement distribution at the bottom of the overlying strata is the same as that at the top of the aquifer; the horizontal displacement and subsidence at the bottom of the overlying strata are therefore also given by $\overline{u}(\zeta, H_w)$ and $\overline{w}(\zeta, H_w)$, respectively. Therefore, the problem of determining the surface movement and deformation caused by pumping is transformed into the problem of determining the surface movement and deformation with a known displacement at the bottom of the overlying strata.

We focus on the overlying strata. If the surface does not bear loads

$$\overline{\sigma}(\zeta, 0) = 0 \qquad \overline{\tau}(\zeta, 0) = 0 \tag{2.11}$$

the corresponding surface movement deformation can then be obtained as follows by substituting Eq. (2.11) into Eq. (2.1)

$$\left\{ \begin{array}{l} \overline{u}(\zeta,0) \\ \overline{w}(\zeta,0) \end{array} \right\} = \left[\begin{array}{cc} \dfrac{B_{22}}{B_{11}B_{22}-B_{21}B_{12}} & \dfrac{-B_{12}}{B_{11}B_{22}-B_{21}B_{12}} \\ \dfrac{B_{11}}{B_{11}B_{22}-B_{21}B_{12}} & \dfrac{-B_{21}}{B_{11}B_{22}-B_{21}B_{12}} \end{array} \right] \left\{ \begin{array}{l} \overline{w}(\zeta,H_w) \\ \overline{u}(\zeta,H_w) \end{array} \right\} \tag{2.12}$$

where the matrix coefficients are given by

$$\begin{aligned} B_{11} &= \cosh m + \frac{m\sinh m}{2(1-\mu_1)} \qquad B_{12} = \frac{1}{2(1-\mu_1)}[(1-2\mu_1)\sinh m + m\cosh m] \\ B_{21} &= \frac{1}{2(1-\mu_1)}[(1-2\mu_1)\sinh m - m\cosh m] \qquad B_{22} = \cosh m - \frac{m\sinh m}{2(1-\mu_1)} \end{aligned} \tag{2.13}$$

where $m = \zeta H_w$ and μ_1 is Poisson's ratio of the overlying strata.

Equation (2.9) is substituted into Eq. (2.12) to obtain the surface movement deformation as follows

$$\begin{aligned} \overline{u}(\zeta,0) &= \Big(\frac{B_{22}}{B_{11}B_{22}-B_{21}B_{12}}\Big)\Big(-\frac{A_{22}A_{13}-A_{12}A_{23}}{A_{11}A_{22}-A_{12}A_{21}}\Big)\frac{\overline{\sigma}_z(\zeta,H_w)}{E_2}H_0 \\ &\quad + \Big(\frac{-B_{12}}{B_{11}B_{22}-B_{21}B_{12}}\Big)\Big(\frac{A_{21}A_{13}-A_{11}A_{23}}{A_{11}A_{22}-A_{12}A_{21}}\Big)\frac{\overline{\sigma}_z(\zeta,H_w)}{E_2}H_0 \\ \overline{w}(\zeta,0) &= \Big(\frac{B_{11}}{B_{11}B_{22}-B_{21}B_{12}}\Big)\Big(\frac{A_{21}A_{13}-A_{11}A_{23}}{A_{11}A_{22}-A_{12}A_{21}}\Big)\frac{\overline{\sigma}_z(\zeta,H_w)}{E_2}H_0 \\ &\quad + \Big(\frac{-B_{21}}{B_{11}B_{22}-B_{21}B_{12}}\Big)\Big(-\frac{A_{22}A_{13}-A_{12}A_{23}}{A_{11}A_{22}-A_{12}A_{21}}\Big)\frac{\overline{\sigma}_z(\zeta,H_w)}{E_2}H_0 \end{aligned} \tag{2.14}$$

By simplifying the coefficients in Eq. (2.14), we obtain

$$\overline{u}(\zeta,0) = (C_1+C_2)\frac{\overline{\sigma}_z(\zeta,H_w)}{E_2}H_0 \qquad \overline{w}(\zeta,0) = (C_3+C_4)\frac{\overline{\sigma}_z(\zeta,H_w)}{E_2}H_0 \tag{2.15}$$

where the coefficients are given by

$$\begin{aligned} C_1 &= \Big(\frac{B_{22}}{B_{11}B_{22}-B_{21}B_{12}}\Big)\Big(-\frac{A_{22}A_{13}-A_{12}A_{23}}{A_{11}A_{22}-A_{12}A_{21}}\Big) \\ C_2 &= \Big(\frac{-B_{12}}{B_{11}B_{22}-B_{21}B_{12}}\Big)\Big(\frac{A_{21}A_{13}-A_{11}A_{23}}{A_{11}A_{22}-A_{12}A_{21}}\Big) \\ C_3 &= \Big(\frac{B_{11}}{B_{11}B_{22}-B_{21}B_{12}}\Big)\Big(\frac{A_{21}A_{13}-A_{11}A_{23}}{A_{11}A_{22}-A_{12}A_{21}}\Big) \\ C_4 &= \Big(\frac{-B_{21}}{B_{11}B_{22}-B_{21}B_{12}}\Big)\Big(-\frac{A_{22}A_{13}-A_{12}A_{23}}{A_{11}A_{22}-A_{12}A_{21}}\Big) \end{aligned} \tag{2.16}$$

The Hankel integral inverse transformation is performed on the expressions in Eq. (2.15) to obtain the surface movement deformation caused by pumping from the confined aquifer

$$\begin{aligned} u(r,0) &= \int_0^\infty (C_1+C_2)\frac{\overline{\sigma}_z(\zeta,H_w)}{E_2}H_0\zeta J_1(\zeta r)\,d\zeta \\ w(r,0) &= \int_0^\infty (C_3+C_4)\frac{\overline{\sigma}_z(\zeta,H_w)}{E_2}H_0\zeta J_0(\zeta r)\,d\zeta \end{aligned} \tag{2.17}$$

Equation (2.17) implies that the surface movement and deformation caused by pumping from a confined aquifer are closely dependent on the thickness, elastic modulus, and Poisson's ratio of the strata and the stress distribution in the aquifer caused by pumping. Compared with the traditional probability integral models, more influencing factors are considered in our layer mechanics model. The total surface movement deformation caused by simultaneous pumping of multiple aquifers can be obtained by using our model to calculate the surface movement deformation caused by pumping from each confined aquifer and then summing the movement deformations caused by pumping over all the aquifers using the superposition principle.

3. Model validation

To verify the accuracy and rationality of the theoretical model, the confined aquifer pumping in Dezhou City, Shandong Province, China in the reference (Jia *et al.*, 2021) was taken as an example. The geological distribution of the study area is shown in Fig. 3, and the physical and mechanical parameters are listed in Table 1. The surface movement and deformation caused by extraction of the same volume of water from two confined aquifers at a pumping capacity of 2441.66 m^3/d, pumping well radius of 1 m, and water density of 10 kN/m^3 were simulated in the reference (Jia *et al.*, 2021). Based on the data provided in the reference, our theoretical model was used to independently calculate the surface subsidence deformation caused by pumping from the two confined aquifers under the same pumping conditions and the results compared with those from the simulation. The results are shown in Fig. 4.

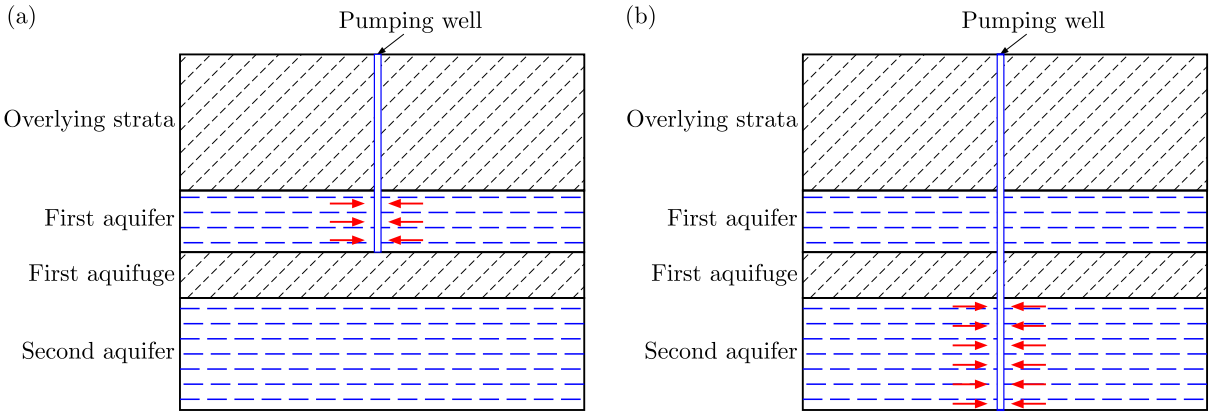

Fig. 3. Schematic of pumping from confined aquifers

Table 1. Calculation parameters

Stratum	Thickness [m]	E [MPa]	k [m/d]	μ	R [km]
Overlying strata	300	80	0.008	0.35	
First aquifer	150	120	1.8	0.25	2.0
First aquifuge	100	60	0.005	0.25	
Second aquifer	250	190	1.5	0.20	1.5

As shown in Fig. 4, the surface subsidence caused by pumping from a confined aquifer is symmetrically distributed with respect to the pumping well. The subsidence is larger closer to the pumping well. The theoretical curves for the surface subsidence caused by separate pumping of the same volume of water from the two confined aquifers are basically the same as the simulation curves. The high consistency of the theoretical calculation subsidence results with the simulation results verifies the correctness of the theoretical model.

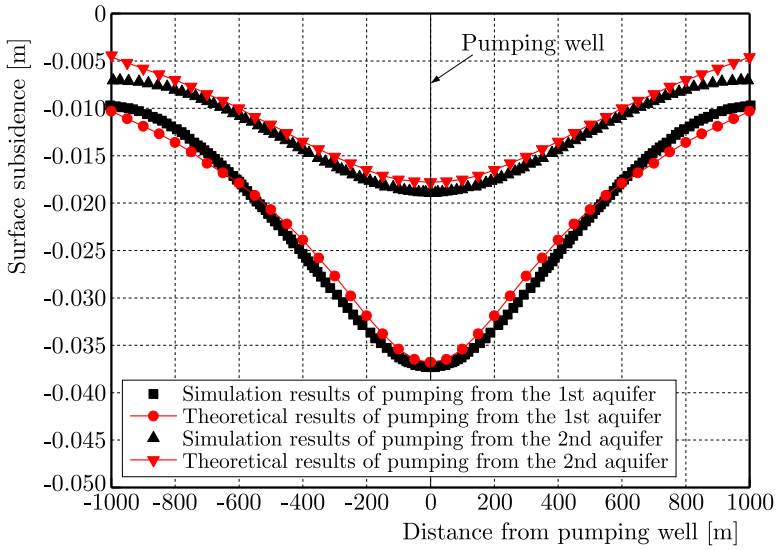

Fig. 4. Comparison of theoretical calculation and numerical simulation results

The maximum surface subsidence caused by individual pumping of the first confined aquifer in the simulation is 0.037 m while that in the theoretical calculation is 0.036 m. The error between them is only 0.01 m. The maximum surface subsidence caused by independent pumping of the second confined aquifer in the simulation is 0.019 m while that in the theoretical calculation is 0.018 m. The error of only 0.01 m between the two results indicates that the maximum surface subsidence in the theoretical calculation is essentially the same as that in the simulation. At a distance of 1000 m from the pumping well, the simulation values for the surface subsidence caused by the separate pumping of the first and second confined aquifers are 0.0097 and 0.0071 m, respectively, while the theoretically calculated values are 0.0103 and 0.0046 m, respectively. The respective errors of only 0.0006 and 0.0025 m are negligible. These error analysis results further confirm that the layered mechanics calculation for the surface subsidence caused by pumping of confined aquifers is reasonable and feasible.

4. Analysis of influencing factors

The first confined aquifer in Dezhou City, Shandong Province, China is taken as an example in this study for analyzing the effects of different pumping capacities and aquifer elastic moduli and thicknesses on the surface subsidence and horizontal displacement.

4.1. Pumping capacity

Equation (2.17) was used to calculate the surface subsidence and horizontal displacement at the pumping capacities of 1500, 2000, and 2500 m^3/d for a confined 150 m-thick aquifer with an elastic modulus of 120 MPa and overlying strata thickness of 300 m. The results are shown in Fig. 5.

The surface subsidence curve in Fig. 5a shows that the surface subsidence caused by pumping increases with the pumping capacity and is symmetrically distributed around the pumping well. The maximum surface subsidence occurs at the wellhead and gradually decreases along both its sides. At the pumping capacities of 1500, 2000, and 2500 m^3/d, the maximum surface subsidence values are 0.0226, 0.0302, and 0.0377 m, respectively, which correspond to increases of 0.0076 and 0.0075 m as the pumping capacity grows. At a distance of 1000 m from the pumping well, the surface subsidence for the three pumping capacities are 0.0063, 0.0085, and 0.0106 m, respectively, which correspond to increaments of 0.0022 and 0.0021 m as the pumping capacity grows.

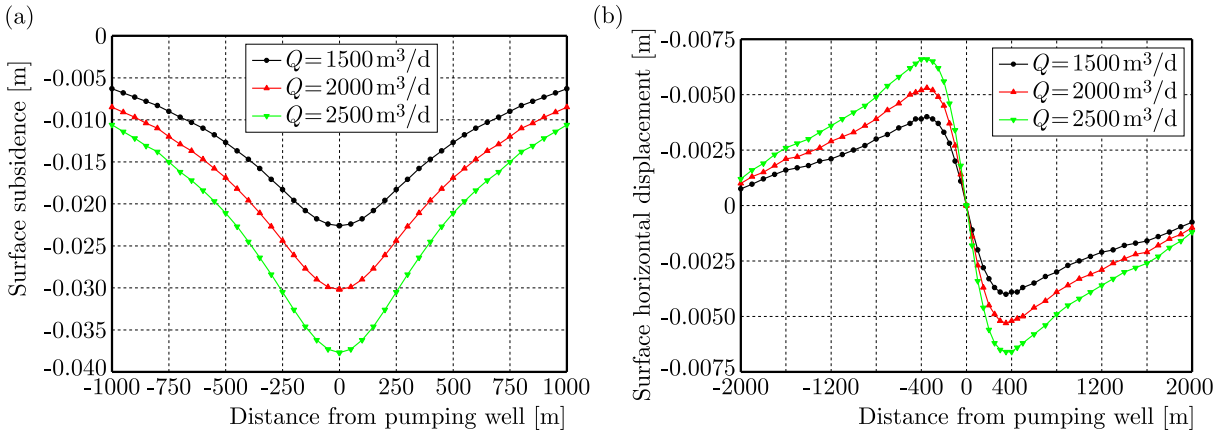

Fig. 5. Relationship between pumping capacity, surface movement, and deformation

These results indicate that increasing the pumping capacity causes a relatively uniform increase in the surface subsidence; however, the growth in the surface subsidence gradually decreases with increasing distance.

The surface horizontal displacement curve in Fig. 5b shows that the surface horizontal displacement caused by exploitation of the confined aquifer increases with the pumping capacity, and its shape is similar to that of a sine function. The surface horizontal displacement at the wellhead is approximately 0. The surface horizontal displacement gradually increases up to a range of approximately 310 m from the pumping well before decreasing with growing distance from the pumping well. Therefore, the maximum surface horizontal displacement occurs approximately 310 m away from the pumping well. For the pumping capacities of 1500, 2000, and 2500 m^3/d, the maximum surface horizontal displacements are 0.0040, 0.0053, and 0.0066 m, respectively, which correspond to increaments of 0.0013 and 0.0013 m. At a distance of 2000 m from the pumping well, the surface horizontal displacements are 0.0007, 0.0010, and 0.0012 m, respectively, which correspond to increaments of 0.0003 and 0.0002 m. These results indicate that increasing the pumping volume causes a relatively uniform growth in the horizontal displacement. The surface horizontal displacement is more sensitive to the pumping capacity nearer the pumping well. Figure 6 also shows that the surface subsidence is larger than the horizontal displacement, but the influence range of the latter is larger.

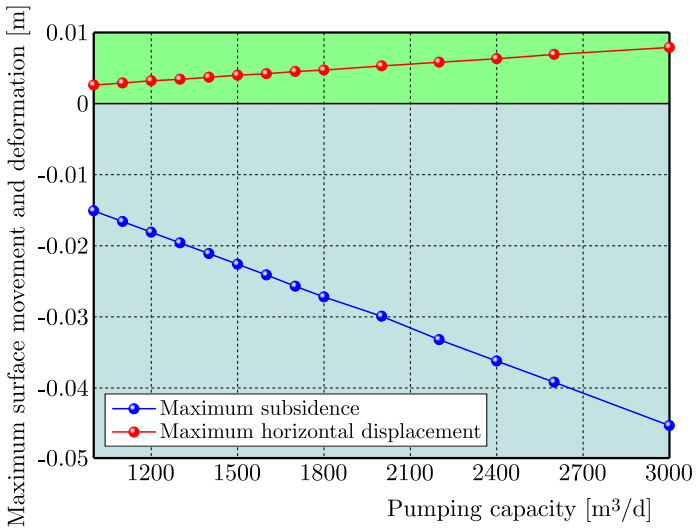

Fig. 6. Relationship between the maximum surface movement deformation and pumping capacity

Figure 6 shows the relationship between the maximum surface subsidence and horizontal displacement, and the pumping capacity. The maximum surface subsidence and horizontal displacement both increase linearly with the pumping capacity. As the pumping capacity increases from 1000 to 3000 m^3/d, the maximum surface subsidence increases from 0.0151 to 0.0453 m while the maximum surface horizontal displacement grows from 0.0026 to 0.0079 m. A higher pumping capacity results in a larger water level drop in the confined aquifer, which leads to a greater additional load acting on the interface between the top of the confined aquifer and the overlying strata. According to layered mechanics, the additional load results in a larger deformation of the confined aquifer, which is transmitted to the surface through the overlying strata and results in more significant surface movement and deformation.

4.2. Confined aquifer elastic modulus

Equation (2.17) was used to calculate the surface subsidence and horizontal displacement at the elastic modulus of 60, 90, and 120 MPa for a confined 150 m-thick aquifer with pumping capacities of 2441.66 m^3/d and overlying strata thickness of 300 m. The results are shown in Fig. 7.

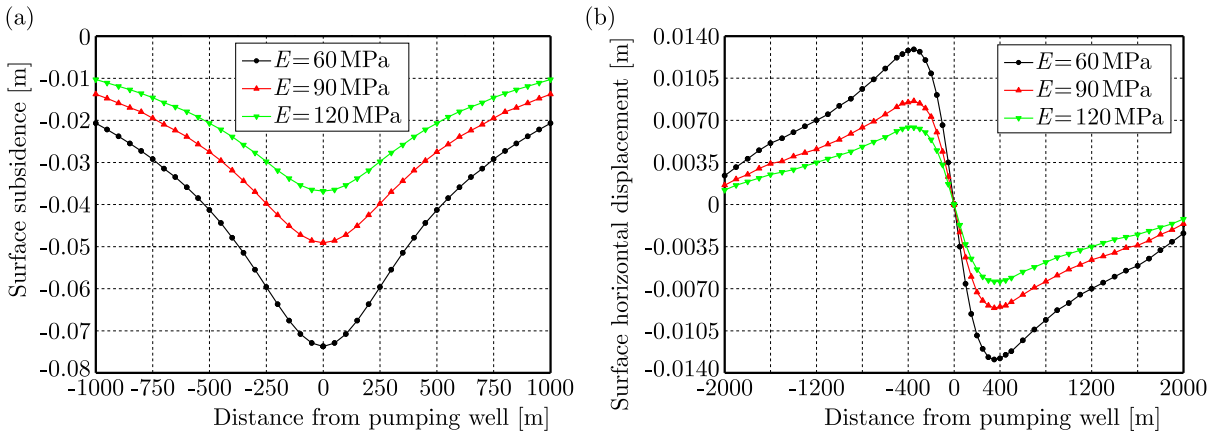

Fig. 7. Relationship between the elastic modulus, surface movement, and deformation

The surface subsidence curve in Fig. 7a shows that the surface subsidence caused by pumping decreases with the elastic modulus. At the elastic modulus of 60, 90, and 120 MPa, the maximum surface subsidence values are 0.0737, 0.0491, and 0.0368 m, respectively, which correspond to decreaments of 0.0246 and 0.0123 m as the elastic modulus increases. At a distance of 1000 m from the pumping well, the surface subsidence values for the three elastic modulus are 0.0207, 0.0138, and 0.0103 m, respectively, which correspond to decreaments of 0.0069 and 0.0035 m as the elastic modulus increases. These results indicate that increasing the elastic modulus causes a relatively uniform decrease in the surface subsidence.

The surface horizontal displacement curve in Fig. 7b shows that the surface horizontal displacement caused by the exploitation of the confined aquifer decreases with the elastic modulus, and its shape is similar to that of a sine function. The maximum surface horizontal displacement also occurs approximately 310 m away from the pumping well. For the elastic modulus of 60, 90, and 120 MPa, the maximum surface horizontal displacements are 0.0129, 0.0086, and 0.0064 m, respectively, which correspond to decreaments of 0.0043 and 0.0022 m. At a distance of 2000 m from the pumping well, the surface horizontal displacements are 0.0024, 0.0016, and 0.0012 m, respectively, which correspond to decreaments of 0.0008 and 0.0004 m. These results indicate that increasing the elastic modulus causes a smaller decrease in the surface horizontal displacement. The surface horizontal displacement is more sensitive to the elastic modulus nearer the pumping well.

Figure 8 shows the relationship between the maximum surface subsidence and horizontal displacement, and the elastic modulus. The maximum surface subsidence and horizontal displacement both decrease nonlinearly with the elastic modulus. As the elastic modulus increases from 10 to 200 MPa, the maximum surface subsidence decreases from 0.4423 to 0.0221 m while the maximum surface horizontal displacement decreases from 0.0772 to 0.0039 m. According to layered mechanics, a higher elastic modulus results in a smaller deformation of the confined aquifer, which is transmitted to the surface through the overlying strata and results in less significant surface movement and deformation.

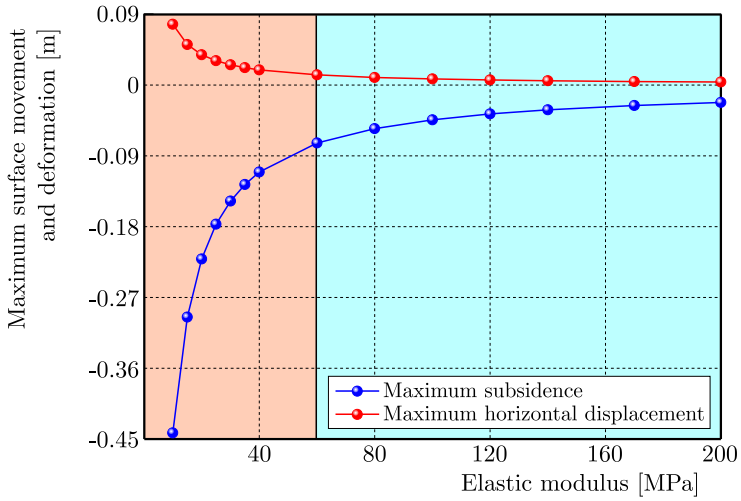

Fig. 8. Relationship between the maximum surface movement deformation and elastic modulus

4.3. Confined aquifer thickness

Equation (2.17) was used to calculate the surface subsidence and horizontal displacement at the thickness of 50, 100, and 150 m for a confined 2441.66 m^3/d – pumping capacities aquifer with an elastic modulus of 120 MPa and overlying strata thickness of 300 m. The results are shown in Fig. 9.

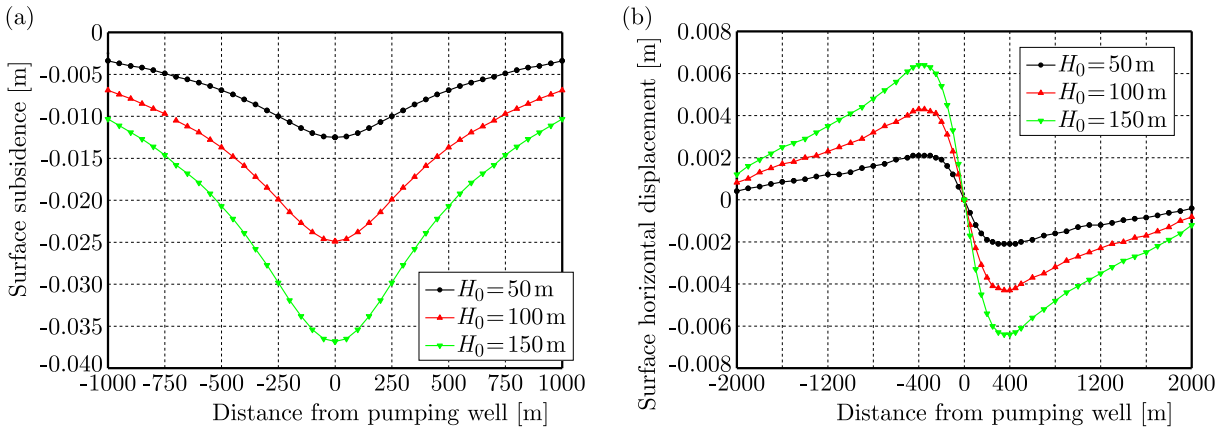

Fig. 9. Relationship between thicknesses, surface movement, and deformation

The surface subsidence curve in Fig. 9a shows that the surface subsidence caused by pumping increases with the aquifer thickness. At the aquifer thickness of 50, 100, and 150 m, the maximum surface subsidence values are 0.0125, 0.0249, and 0.0368 m, respectively, which correspond to increaments of 0.0124 and 0.0119 m as the aquifer thickness increases. At a distance of 1000 m

from the pumping well, the surface subsidence values for the three aquifer thickness are 0.0034, 0.0069, and 0.0103 m, respectively, which correspond to increaments of 0.0035 and 0.0034 m as the aquifer thickness increases. These results indicate that increasing the aquifer thickness causes a relatively uniform increase in the surface subsidence.

According to the surface horizontal displacement curve in Fig. 9b, it can be seen that the surface horizontal displacement caused by exploitation of the confined aquifer increases with a growth of aquifer thickness, and the maximum surface horizontal displacement occurs about 310 m away from the pumping well. When the thickness of the aquifer is 50, 100, and 150 m, respectively, the maximum surface horizontal displacement is 0.0021, 0.0043, and 0.0064 m, with increaments of 0.0022 m and 0.0021 m, respectively. At a distance of 2000 m from the pumping well, the surface horizontal displacement is 0.0004, 0.0008, and 0.0012, respectively, with increaments of 0.0004 m and 0.0004 m, indicating that the increase in thickness of the aquifer causes a relatively uniform increase in surface horizontal displacement, and the elastic modulus of the aquifer is more sensitive to surface horizontal displacement near the pumping well than in the distance.

The surface horizontal displacement curve in Fig. 10b shows that the surface horizontal displacement caused by the exploitation of the confined aquifer increases with the aquifer thickness, and the maximum surface horizontal displacement occurs about 310 m away from the pumping well. For the aquifer thickness of 50, 1000, and 1500 m, the maximum surface horizontal displacements are 0.0021, 0.0043, and 0.0064 m, respectively, which correspond to increaments of 0.0022 and 0.0021 m. At a distance of 2000 m from the pumping well, the surface horizontal displacements are 0.0004, 0.0008, and 0.0012 m, respectively, which correspond to increaments of 0.0004 and 0.0004 m. These results indicate that increasing the aquifer thickness causes a relatively uniform increase in the surface horizontal displacement. The surface horizontal displacement is more sensitive to the pumping capacity nearer the pumping well.

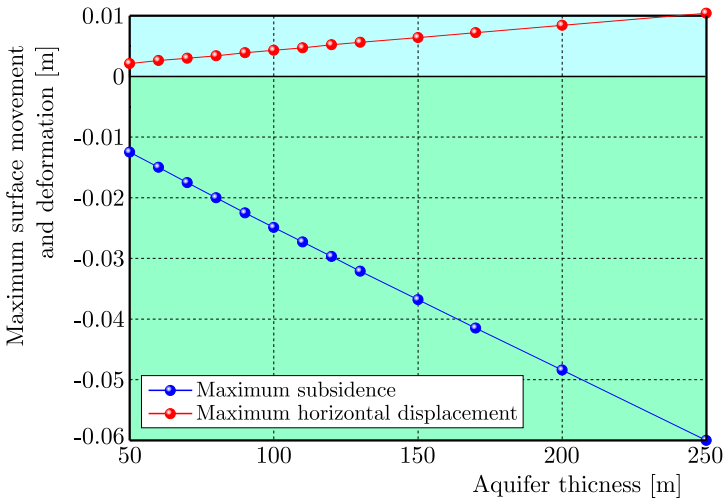

Fig. 10. Relationship between the maximum surface movement deformation and aquifer thickness

Figure 10 shows the relationship between the maximum surface subsidence and horizontal displacement, and the aquifer thickness. The maximum surface subsidence and horizontal displacement both increase linearly with the aquifer thickness. As the aquifer thickness increases from 50 to 250 m, the maximum surface subsidence increases from 0.0125 m to 0.0600 m while the maximum surface horizontal displacement increases from 0.0021 m to 0.0104 m. According to layered mechanics, a thicker aquifer results in a larger deformation of the confined aquifer, which is transmitted to the surface through the overlying strata and results in more significant surface movement and deformation.

5. Maximum displacement position

By analyzing the influencing factors, it was found that under different pumping volume and aquifer elastic modulus and thickness conditions, the maximum surface subsidence occurs at the wellhead, and the maximum horizontal displacement occurs at a distance of approximately 310 m from the pumping well. This indicates that the above influencing factors affect only the numerical value and range of the surface displacement deformation but not the position where the maximum surface displacement deformation occurs. Taking the first confined aquifer in Dezhou City as an example, the relationship between the position of the maximum surface horizontal displacement and the thickness of the overlying strata was analyzed. The results are shown in Fig. 11.

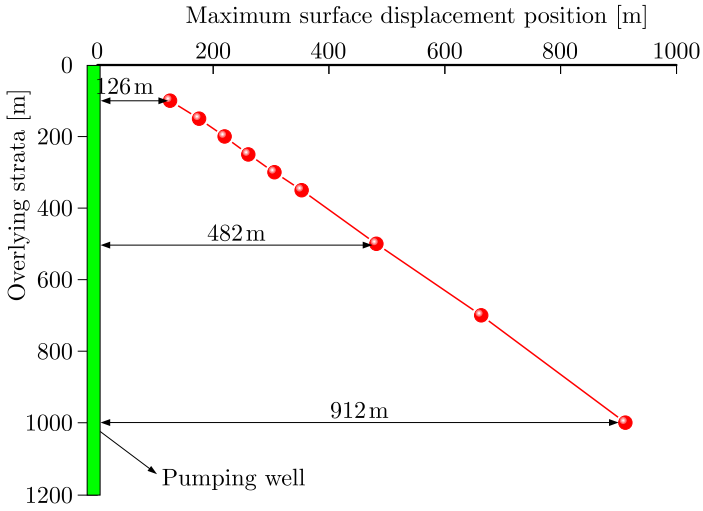

Fig. 11. Relationship between the maximum surface horizontal displacement position and overlying strata thickness

As shown in Fig. 11, the distance between the position of the maximum surface horizontal displacement and the pumping well increases linearly with the thickness of the overlying strata. At the overlying strata thicknesses of 100, 500, and 1000 m, the maximum surface horizontal displacements occur 126, 482, and 912 m away from the pumping well, respectively. The distance between the maximum surface horizontal displacement position and the pumping well increases with the thickness of the overlying strata at a rate of 0.87. In other words, for every 1 m increase in the thickness of the overlying strata, the maximum surface horizontal displacement occurs a further 0.87 m away from the pumping well. In contrast, the maximum surface subsidence occurs at the wellhead regardless of the aquifer or overlying strata parameters because the maximum water level drop caused by pumping in the confined aquifer occurs at the wellhead.

6. Discussion

Based on the principle of coordinated strata deformation, the paper uses the theory of layered mechanics to establish a calculation model for surface movement and deformation caused by pumping in confined aquifers. Compared with the consolidation theory model and the probability integration method in the calculation model, the model in this paper can consider not only the surface deformation within the range of pumping influence, but also reflect the influence of geological physical and mechanical parameters on surface movement and deformation. The theoretical model can comprehensively consider such factors as aquifer thickness, elastic modulus, pumping capacity, and overlying strata thickness, and is more reasonable compared to the

existing computational models. By comparing with the monitoring data of surface deformation caused by pumping wells in Dezhou City, China, it is shown that the model is suitable for calculating surface movement and deformation caused by pumping in confined aquifers, and it also demonstrates that the model has high accuracy.

What is more, the theoretical model proposed in this paper is mainly used to calculate surface movement and deformation caused by pumping in confined aquifers, and has good applicability and high accuracy. However, in the field of coal resource extraction, surface movement and deformation often occur due to disturbances caused by coal mining, surface pumping, surface grouting, and other factors that affect the water level of the aquifer (Tajdus *et al.*, 2023; Dudek *et al.*, 2020), thereby affecting safety of surface buildings. The theoretical model in this paper is applicable for calculating surface movement and deformation caused by the above factors although still needs further modification and improvement.

7. Conclusion

(1) The effective stress increase caused by pumping from a confined aquifer is equivalent to an additional load acting on the top of the aquifer. A model for surface movement and deformation caused by pumping from a confined aquifer was established using layered mechanics in which the effects of the aquifer thickness, elastic modulus, pumping volume, and overlying strata thickness are considered. The consistency of the results for the surface subsidence caused by extraction of confined aquifers in Dezhou City, Shandong Province, China obtained using the model with numerical simulation results verifies the accuracy and rationality of the model.

(2) The surface subsidence and horizontal displacement caused by confined aquifer extraction are positively correlated with the pumping volume and aquifer thickness and negatively correlated with the aquifer elastic modulus. The maximum surface subsidence and horizontal displacement increase linearly with the pumping volume and aquifer thickness, and decrease nonlinearly with the increasing aquifer elastic modulus.

(3) The maximum surface subsidence caused by pumping from a confined aquifer occurs at the wellhead. The position of the maximum horizontal displacement is independent of the pumping volume, elastic modulus, and aquifer thickness. The distance between the position of the maximum horizontal displacement and the pumping well increases linearly with the thickness of the overlying strata.

Acknowledgments

This research was financially supported by the Natural Science Research Project of Anhui Educational Committee (Grant Numbers: 2023AH051203), the Scientific Research Start Funds of Anhui University of Science and Technology (Grant Numbers: 2022yjrc32), the National Natural Science Foundation of China (Grant Numbers: 52404069). The authors would like to thank the editor and reviewers for their contributions on the paper.

References

1. Abidin H.Z., Andreas H., Gumilar I., Fukuda Y., Pohan Y.E., Deguchi T., 2011, Land subsidence of Jakarta (Indonesia) and its relation with urban development, *Natural Hazards*, **59**, 3, 1753-1771

2. Bobileva T.N., 2017, Stress distribution in the stratified mass containing vertical alveole (in Russian), *Vestnik MGSU*, **12**, 8(107), 863-868

3. Bourel C., 2024, Water flow in shallow aquifers without the Dupuit hypothesis, *Computers and Mathematics with Applications*, **163**, 165-185

4. Cheng H., Zhang L.L., Yao Z.S., Peng S.L., Guo L.H., 2022, Mechanism of shaft deflection caused by asymmetric mining in thin bedrock and deep loose strata (in Chinese), *Journal of China Coal Society*, **47**, 1, 102-114

5. Cui Z.D., Tang Y.Q., 2007, Domestic and international recent situation and research of land subsidence disasters (in Chinese), *China Earthquake Engineering Journal*, **29**, 3, 275-278

6. Dudek M., Tajdus K., Misa R., Sroka A., 2020, Predicting of land surface uplift caused by the flooding of underground coal mines – A case study, *International Journal of Rock Mechanics and Mining Sciences*, **132**, 104377

7. Galloway D.L., Burbey T.J., 2011, Review: Regional land subsidence accompanying groundwater extraction, *Hydrogeology Journal*, **19**, 8, 1459-1486

8. Gamnitzer P., Hofstetter G., 2016, Fully coupled multi-phase modelling of pumping induced settlements, air- and water flow in multi-layered normally consolidated soils, *Computers and Geotechnics*, **79**, 10-21

9. Giang N.V., 2022, Application of artificial storage, recharge for semi-arid area in BacBinh Vietnam, *Archives of Mining Sciences*, **67**, 1, 37-53

10. Giao P.H., 1997, Artificial recharge of the Bangkok aquifer system for the mitigation of land subsidence, Dissertation No. GE-96-2, Asian Institute of Technology (AIT), Bangkok

11. Guido L., Libera E., Francesco F., 2023, Terzaghi's effective stress principle and hydrological deformation of Karst aquifers detected by GNSS measurements, *Rock Mechanics and Rock Engineering*, **57**, 4, 2365-2383

12. Holzer T.L., Johnson A.I., 1985, Land subsidence caused by ground water withdrawal in urban areas, *GeoJournal*, **11**, 3, 245-255

13. Jia C., Di S.T., Sun X.X., Zhang S.P., Ding P.P., Liu Z.T., 2021, Spatiotemporal evolution characteristics and transfer law of land subsidence in sand-clay interbed caused by exploiting the groundwater, *Arabian Journal for Science and Engineering*, **46**, 6, 5733-5753

14. Jia Y.J., Liang F.Y., Cui Z.D., Ye H., 2016, Analysis of soil deformation caused by decompression of confined water based on displacement coordination condition (in Chinese), *Rock and Soil Mechanics*, **37**, 42-48

15. Li M.G., Chen J.J., Xu Y.S., Tong D.G., Cao W.W., Shi Y.J., 2021, Effects of groundwater exploitation and recharge on land subsidence and infrastructure settlement patterns in Shanghai, *Engineering Geology*, **282**, 105995

16. Liu Z., Song Y., Zhou F., Wang L., 2023, Analytical solution for one-dimensional consolidation of unsaturated soils under dynamic load, *Journal of Theoretical and Applied Mechanics*, **61**, 1, 11-22

17. Loáiciga H.A., 2013, Consolidation settlement in aquifers caused by pumping, *Journal of Geotechnical and Geoenvironmental Engineering*, **139**, 7, 1191-1204

18. Malinowska A., Hejmanowski R., Dai H., 2020, Ground movements modeling applying adjusted influence function, *International Journal of Mining Science and Technology*, **30**, 2, 243-249

19. Motagh M., Shamshiri R., Haghighi M.H., Wetzel H.U., Akbari B., *et al.*, 2017, Quantifying groundwater exploitation induced subsidence in the Rafsanjan plain, southeastern Iran, using InSAR time-series and in situ measurements, *Engineering Geology*, **218**, 134-151

20. Ortega-Guerrero A., Rudolph D.L., Cherry J.A., 1999, Analysis of long-term land subsidence near Mexico City: field investigations and predictive modeling, *Water Resources Research*, **35**, 11, 3327-3341

21. Peng S., Li Z., Xu Y., Cao G., 2023, Study on the nonlinear permeability mechanism and pore structure characteristics of deep confined aquifers, *Applied Sciences*, **13**, 20, 11599

22. Szojda L., Kapusta L., 2023, Numerical analysis of buildings located on the edge of the post--mining basin, *Archives of Mining Sciences*, **68**, 1, 125–140

23. Tajdus K., Sroka A., Dudek M., Misa R., Hager S., Rusek J., 2023, Effect of the entire coal basin flooding on the land surface deformation, *Archives of Mining Sciences*, **68**, 3, 375-392

24. Tang F.Q., Bai F., 2011, Calculation method of surface subsidence caused by water loss in thick loess mining area (in Chinese), *Journal of Xian University of Science and Technology*, **31**, 4, 448-452

25. Wang X.W., Yang T.L., Xu Y.S., Shen S.L., 2019, Evaluation of optimized depth of waterproof curtain to mitigate negative impacts during dewatering, *Journal of Hydrology*, **577**, 123969

26. Xu Y.S., Yuan Y., Shen S.L., Yin Z.Y., Wu H.N., Ma L., 2015, Investigation into subsidence hazards due to groundwater pumping from Aquifer II in Changzhou, China, *Natural Hazards*, **78**, 1, 281-296

27. Zhou N.Q., Vermeer P.A., Lou R.X., Tang Y.Q., Jiang S., 2010, Numerical simulation of deep foundation pit dewatering and optimization of controlling land subsidence, *Engineering Geology*, **114**, 3-4, 251-260

Manuscript received July 10, 2024; accepted for publication November 7, 2024